ARTICLE

Immobilization of Biomolecules on the Surface of Electrospun Polycaprolactone Fibrous Scaffolds for Tissue Engineering

Waradda Mattanavee,[†] Orawan Suwantong,[‡] Songchan Puthong,[§] Tanom Bunaprasert,[∥] Voravee P. Hoven,[⊥] and Pitt Supaphol*[,‡]

Program of Petrochemistry and Polymer Science, Faculty of Science, The Petroleum and Petrochemical College and The Center for Petroleum, Petrochemicals and Advanced Materials, The Institute of Biotechnology and Genetic Engineering, Department of Otolaryngology Head and Neck Surgery, Faculty of Medicine, and Organic Synthesis Research Unit, Department of Chemistry, Faculty of Science, Chulalongkorn University, Bangkok 10330, Thailand

ABSTRACT To make polycaprolactone (PCL) more suitable for tissue engineering, PCL in the form of electrospun fibrous scaffolds was first modified with 1,6-hexamethylenediamine to introduce amino groups on their surface. Various biomolecules, i.e., collagen, chitosan, and Gly-Arg-Gly-Asp-Ser (GRGDS) peptide, were then immobilized on their surface, with *N*,*N*′-disuccinimidylcarbonate being used as the coupling agent. Dynamic water contact angle measurement indicated that the scaffold surface became more hydrophilic after the aminolytic treatment and the subsequent immobilization of the biomolecules. The appropriateness of these PCL fibrous scaffolds for the tissue/cell culture was evaluated in vitro with three different cell lines, e.g., mouse fibroblasts (L929), human epidermal keratinocytes (HEK001), and mouse calvaria-derived preosteoblastic cells (MC3T3-E1). Both the neat and the modified PCL fibrous scaffolds released no substances in the levels that were harmful to these cells. Among the various biomolecule-immobilized PCL fibrous scaffolds, the ones that had been immobilized with type I collagen, a Arg-Gly-Asp-containing protein, showed the greatest ability to support both the attachment and the proliferation of all of the investigated cell types, followed by those that had been immobilized with GRGDS peptide.

KEYWORDS: electrospinning • polycaprolactone • immobilization • collagen • chitosan • GRGDS

1. INTRODUCTION

Tissue engineering is an interdisciplinary technology that combines knowledges from materials engineering, cellular biology, and genetic engineering to bring about artificial tissues or organs, such as skin, cartilage for joints, heart valves, bone, etc. A functional scaffold for tissue engineering must support and define the three-dimensional organization of the tissue-engineered space and, at the same time, maintain the normal differentiated state of the cells within the cellular compartment. Ideally, a functional scaffold should be able to mimic the structure and biological function of the native extracellular matrix (ECM) proteins, so as to provide mechanical support and regulate cellular activities (1). Because of the high surface area to volume or mass ratio and the vast possibilities for surface functionalization, fibers in the form of nonwoven membranes as obtained by the process known as electrospinning have recently become the most studied form of tissue-engineered scaffolds (2).

Over the past decade, the development of scaffolds for cell/tissue culture based on the use of biodegradable and biocompatible synthetic or natural polymers has been emphasized (3−7). Polycaprolactone (PCL), an ideal scaffolding material owing to its biodegradability and biocompatibility, is a semicrystalline polymer with a melting temperature (T_m) of ca. 60 °C and a glass transition temperature (T_g) of ca. −60 °C (8). PCL, approved by the U.S. Food and Drug Administration, has good mechanical properties when biaxially stretched (9). Because of its inherent biodegradability and biocompatibility properties, PCL has been widely explored for its potential use in medicine, such as drug carriers (10), engineered skin (11−13), scaffolds for supporting the growth of fibroblasts and osteoblasts (10, 14), etc. Notwithstanding, its hydrophobicity often leads to unfavorable cell adhesion and growth (15). Therefore, the cytocompatibility of PCL should be further improved.

Surface modification has long been recognized as a potential tool for enhancing the biocompatibility of the surface of a material. Because hydrophilic and protein-containing surfaces are known to promote cellular growth, many researches have focused on immobilizing biomolecules, such as collagen (8, 16−18), gelatin (19, 20), laminin (21−23), chitosan (24−26), Arg-Gly-Asp (RGD)-containing peptide (27, 28), etc., onto the surfaces of polymeric scaffolds to improve their cytocompatibility. The

* Author to whom correspondence should be addressed. E-mail: pitt.s@chula.ac.th.

Received for review January 22, 2009 and accepted April 3, 2009

[†] Program of Petrochemistry and Polymer Science, Faculty of Science.

[‡] The Petroleum and Petrochemical College and The Center for Petroleum, Petrochemicals and Advanced Materials.

[§] The Institute of Biotechnology and Genetic Engineering.

[∥] Department of Otolaryngology Head and Neck Surgery, Faculty of Medicine.

[⊥] Organic Synthesis Research Unit, Department of Chemistry, Faculty of Science.

DOI: 10.1021/am900048t

Published on Web 04/21/2009

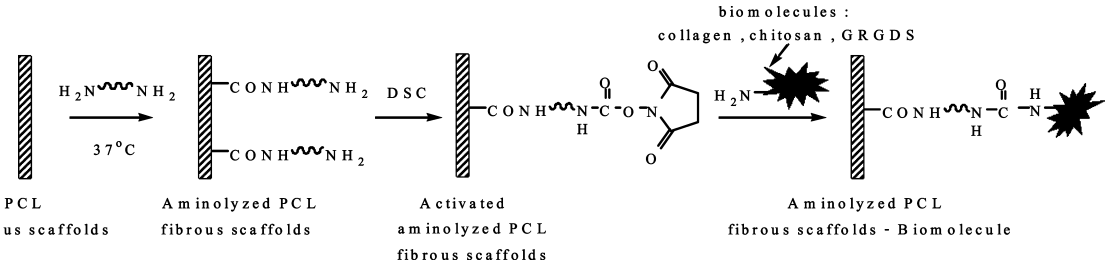

FIGURE 1. Chemical pathway for the immobilization of different biomolecules, such as collagen (i.e., marine collagen, COLM; type I collagen, COLI; type IV collagen, COLIV), chitosan (i.e., CS15, $M_w = 15\ 000\ g \cdot mol^{-1}$; CS83, $M_w = 83\ 000\ g \cdot mol^{-1}$), or GRGDS peptide (i.e., H-Gly-Arg-Cly-Asp-Ser-OH), on the surface of the electrospun PCL fibrous scaffolds.

present contribution focuses on improving the hydrophilicity, and hence the cytocompatibility, of the surface of the electrospun PCL fibrous scaffolds by treatment with 1,6-hexamethylenediamine (HMD) and using the induced amino groups as precursors for subsequent immobilization with three different biomolecules, e.g., collagen, chitosan, and Gly-Arg-Gly-Asp-Ser (GRGDS) peptide. These biomolecules were chosen based on their biological functionalities. Cytocompatibility of the biomolecule-immobilized scaffolds was then assessed in vitro with keratinocytes (HEK001), fibroblasts (L929), and osteoblasts (MC3T3-E1) in terms of cytotoxicity, cell adhesion, and cell proliferation. These different cell lineages were chosen based on the usual proposed uses of PCL as skin and bone prostheses.

2. EXPERIMENTAL SECTION

2.1. Materials. Materials used in the fabrication of the fibrous scaffolds were polycaprolactone (PCL; $M_n = 80\ 000\ g \cdot mol^{-1}$; Aldrich, Madison, WI), dichloromethane (DCM; Carlo Erba, Rodano, Italy), and *N*,*N*′-dimethylformamide [DMF; Labscan Asia, Bangkok, Thailand]. Materials used in the modification of the surface of the PCL fibrous scaffolds were marine collagen (COLM; Ta Ming Enterprises, Samut Sakhon, Thailand), type I collagen (COLI, calf skin; Sigma, Milwaukee, WI), type IV collagen (COLIV, human placenta; Sigma, Milwaukee, WI), chitosan [CS15, $M_w \approx 15\ 000\ g \cdot mol^{-1}$; CS83, $M_w \approx 83\ 000\ g \cdot mol^{-1}$; Seafresh Chitosan (Laboratory), Bangkok, Thailand], H-Gly-Arg-Gly-Asp-Ser-OH peptide (GRGDS peptide; CalBiochem, Merck, Haar, Germany), 1,6-hexamethylenediamine (HMD; Fluka, Buchs, Switzerland), and *N*,*N*′-disuccinimidylcarbonate (DSC; Novabiochem, Merck, Haar, Germany). All other chemicals were of analytical reagent grade and used without further purification.

2.2. Preparation of Electrospun PCL Fibrous Scaffolds. Electrospun PCL fiber mats used as fibrous scaffolds were fabricated by electrospinning from a 12% (w/v) PCL solution in 50:50 (v/v) DCM/DMF. A blunt 20-gauge stainless steel hypodermic needle (o.d. = 0.91 mm) was used as the nozzle. An aluminum sheet wrapped around a rotating cylinder (width and o.d. of the cylinder ≈ 15 cm; rotational speed ≈ 50 rpm) was used as the collector. The distance from the tip of the needle to the surface of the aluminum sheet (measured at a right angle to the surface) defining the collection distance was 10 cm. A Gamma High-Voltage Research D-ES30PN/M692 power supply was used to generate a direct current potential of 21 kV. The emitting electrode of positive polarity was connected to the needle, while the grounding one was connected to the collector. The feed rate of the PCL solution was controlled by a Kd Scientific syringe pump at $1\ mL \cdot h^{-1}$. After continuous spinning for 10 h, the thickness of the obtained PCL fibrous scaffolds was about 130 μm. The morphology of the fibrous scaffolds and the size of the individual fiber segments therein were examined by a JEOL JSM 5410LV scanning electron microscope. At least 100 fiber segments from multiple scanning electron microscopy (SEM) images were statistically analyzed using *SemAphore 4.0* software, from which the mean value of the diameters of the fiber segments within the PCL fibrous scaffolds was determined to be about 0.95 μm (29).

2.3. Surface Modification of PCL Fibrous Scaffolds. The PCL fibrous scaffolds were first immersed in an ethanolic aqueous solution (1:1, v/v) for 2−3 h to cleanse the fiber surface and then washed with a large quantity of deionized water. HMD/isopropyl alcohol (IPA) solutions (i.e., 1−5 M) were used to aminolyze the scaffold surface for 8 h at 37 °C. The aminolyzed PCL fibrous scaffolds were then rinsed with deionized water for 24 h at room temperature to remove unreacted HMD and dried in vacuo at 30 °C until of a constant weight. Immobilization of biomolecules, e.g., collagen, chitosan, or GRGDS peptide, onto the surface of the PCL fibrous scaffolds was carried out by first activating the aminolyzed scaffolds with a 0.1 M DSC/dimethyl sulfoxide solution in the presence of 0.1 M triethylamine for a given time interval at ambient temperature, followed by rinsing the scaffolds with a large quantity of deionized water. The activated, aminolyzed PCL fibrous scaffolds were then immersed in a $5\ mg \cdot mL^{-1}$ collagen/phosphate buffer saline (PBS) solution, a $3\ mg \cdot mL^{-1}$ chitosan/acetic acid solution, or a $7\ mg \cdot mL^{-1}$ GRGDS/PBS solution at ambient temperature for 24 h. The biomolecule-immobilized PCL fibrous scaffolds had to be soaked in a large quantity of deionized water for 24 h (for COLM-, COLI-, COLIV-, and GRGDS-immobilized PCL fibrous scaffolds) or a large quantity of a 1% acetic acid solution, followed by a large quantity of deionized water for 24 h (for CS15- and CS83-immobilized PCL fibrous scaffolds), prior to drying in vacuo. Figure 1 summarizes the chemical pathway for the immobilization of different biomolecules (i.e., collagen, chitosan, or GRGDS peptide) onto the surface of the electrospun PCL fibrous scaffolds.

2.4. Physicochemical Characterization of the Neat and Modified PCL Fibrous Scaffolds. ***Quantification of Amino Groups.*** The amount of amino (NH_2) groups on the surfaces of the aminolyzed and biomolecule-immobilized PCL fibrous scaffolds was quantified by ninhydrin assay. First, the fibrous scaffolds were immersed in a 1 M ninhydrin/ethanol solution for 1 min, followed by heating at 80 °C for 15 min to facilitate the reaction between ninhydrin and the NH_2 groups that might be present on the surfaces of the scaffolds. If a sufficient amount of NH_2 groups is present on the surfaces, the surfaces turn blue. After the absorbed ethanol had been completely evaporated, 1,4-dioxane was added into the tube to dissolve the scaffolds. IPA was then added to stabilize the blue compound. The amount of the NH_2 groups was then quantified by observing the absorbance of the obtained mixture at 538 nm using a Techne Specgene ultraviolet−visible (UV−vis) spectrophotometer against a predetermined calibration curve that had been obtained from HMD solutions in 1,4-dioxane/IPA (1:1, v/v; see the Supporting Information).

Water Contact Angle Measurements. A Ramé-Hart 100-00 contact angle goniometer equipped with a Gilmont syringe and a blunt 24-gauge needle was used to determine the contact angles of water drops on the surfaces of both the neat and modified PCL fibrous scaffolds. The measurements were carried out in air at room temperature. Both dynamic advancing and receding contact angles were recorded as incremental amounts of water were either added to or withdrawn from the water drops. The measurements were carried out in pentuplicate on different areas of each sample.

Chemical Analysis. Chemical functional groups on the surfaces of both the neat and modified PCL fibrous scaffolds were analyzed by a Nicolet Magna 750 Fourier-transformed infrared (FTIR) spectrometer equipped with a liquid-nitrogen-cooled mercury−cadmium−telluride detector at a resolution of 4 cm^{-1} and 128 scans. A single attenuated total reflection (ATR) accessory with 45° germanium (Ge) IRE (Spectra Tech, Oak Ridge, TN) and a variable angle reflection accessory (Seagull, Harrick Scientific, Pleasantville, NY) with a hemispherical Ge IRE were employed for all ATR spectral acquisitions.

2.5. Biological Characterization of the Neat and Modified PCL Fibrous Scaffolds. ***Cell Culture.*** Mouse fibroblasts (L929), human epidermal keratinocytes (HEK001), and mouse calvaria-derived preosteoblastic cells (MC3T3-E1) were used as reference cell lines. L929 were cultured in a RPMI 1640 medium supplemented with 5% fetal bovine serum (FBS), penicillin (100 000 U/L), and streptomycin (100 mg/L). HEK001 were cultured in a keratinocyte-serum-free medium supplemented with human recombinant epidermal growth factor (5 ng/mL), L-glutamine (without bovine pituitary extract and without serum; 2 mM), penicillin (100 000 U/L), and streptomycin (100 mg/L). MC3T3-E1 were cultured in an α-minimal essential medium supplemented with 10% FBS, penicillin (100 000 U/L), and streptomycin (100 mg/L).

Cytotoxicity Evaluation. The indirect cytotoxicity evaluation of both the neat and modified PCL fibrous scaffolds was conducted by an adaptation from the ISO10993-5 standard test method. The specimens (circular disks; about 6 mm in diameter) were prewashed with 70% ethanol for 30 min and washed twice with each respective culture medium containing gentamycin (200 mg/L), penicillin (200 000 U/L), and streptomycin (200 mg/L). Extraction media were prepared by immersing the specimens in each respective medium in wells of a 96-well tissue-culture polystyrene plate (TCPS) for 1, 3, or 7 days. Cells were cultured in wells of another TCPS at a density of 5×10^3 cells/well for L929 and 1×10^4 cells/well for HEK001 and MC3T3-E1, respectively, to allow cell attachment onto the plate. After incubation in 5% CO_2 at 37 °C for 24 h, the culture medium was replaced with each of the as-prepared extraction media and the cells were incubated further for another 24 h. Finally, the viability of the cells cultured with each respective culture medium that had been preincubated in empty wells of TCPS for 1, 3, or 7 days (i.e., controls) and each of the as-prepared extraction media was determined with a 3-(4,5-dimethylthiazol-2-yl)-2,5-diphenyltetrazolium bromide (MTT) assay (30) (see the Supporting Information). The experiments were carried out in triplicate.

Cell Attachment and Cell Proliferation. Both the neat and modified PCL fibrous scaffold specimens (circular disks; about 6 mm in diameter) were sterilized by soaking in 70% ethanol for 30 min and washed twice with each respective culture medium containing gentamycin (200 mg/L), penicillin (200 000 U/L), and streptomycin (200 mg/L). The specimens were then placed in wells of a 96-well TCPS. The reference cells (i.e., 5×10^3 cells/well for L929 and 1×10^4 cells/well for HEK001 and MC3T3-E1) were later cultured on the surfaces of these specimens and in wells of TCPS (i.e., positive controls) and then incubated in 5% CO_2 at 37 °C. For the cell attachment studies, the cells were allowed to attach on the substrates for 12 h. For the cell proliferation studies, the cells, after having been allowed to attach on the substrates for 12 h, were cultured for either 2 or 4 days. At each cell-seeding or cell-culturing time point, the viability of the attached and the proliferated cells was quantified by the MTT assay. The experiments were carried out in triplicate.

Morphological Observation of Cultured Cells. After the culture medium had been removed, the cell-cultured specimens were rinsed twice with 0.2 M PBS and the cells were then fixed with 3% gluteraldehyde/PBS for 30 min. After that, the specimens had been washed twice with PBS, prior to being dehydrated in ethanolic aqueous solutions of varying concentrations (30, 50, 70, and 90%) and then with pure ethanol for 2 min each. The specimens were dried in 100% hexamethyldisilazane [HMDS; also known as bis(trimethylsilyl)amine] for 5 min and later in air after removal of HMDS. Finally, the specimens were mounted on SEM stubs, coated with gold using a JEOL JFC-1100E sputtering device for 3 min, and observed by a JEOL JSM-5200 scanning electron microscope.

2.6. Statistical Analysis. Values are expressed as the means ± standard errors of means. Statistical analysis of different data groups was performed using One-Way Analysis of Variance (ANOVA) with the least-significant difference test using *SPSS* software version 12. The values of p lower than 0.01 and 0.05 were considered statistically significant.

Table 1. Areal Density of Amino Groups on the Surface of the Aminolyzed PCL Fibrous Scaffolds as a Function of the HMD Concentration and the Resulting Advancing and Receding Water Contact Angles of the Surfaces[a]

		water contact angle		
HMD concn (M)	NH_2 concn × 10^{-8} (mol · cm^{-2})	advancing (deg)	receding (deg)	hysteresis (deg)
0		142 ± 2	86 ± 2	56
1	0.20 ± 0.04	138 ± 3	83 ± 2	55
2	0.52 ± 0.06	133 ± 2	81 ± 2	52
3	0.67 ± 0.05	130 ± 2	77 ± 2	52
4	1.22 ± 0.02	124 ± 2	71 ± 2	53
5	1.28 ± 0.06	125 ± 2	72 ± 2	53

[a] Aminolyzing time = 8 h.

3. RESULTS AND DISCUSSION

Amino groups can be covalently introduced onto the surface of the electrospun PCL fibrous scaffolds by first reacting the fibrous scaffolds with HMD to obtain the aminolyzed PCL fibrous scaffolds, provided that one amino group (−NH_2) of HMD reacts with the ester group (−COO−) of PCL to form an amide linkage (−CONH−), leaving the other amino group for subsequent reaction. The aminolyzed PCL fibrous scaffolds were then activated with DSC via reaction with the free amino group, with *N*-hydroxysuccinimide being cleaved from the reaction. Biomolecules (i.e., collagen, chitosan, or GRGDS peptide) were finally immobilized onto the surface of the activated, aminolyzed PCL fibrous scaffolds to obtain the biomolecule-immobilized PCL fibrous scaffolds, with *N*-hydroxysuccinimide again being cleaved from the reaction.

3.1. Physicochemical Characterization of the Neat and Modified PCL Fibrous Scaffolds. To assess the degree of aminolysis, ninhydrin was used to determine the amount of free amino groups introduced on the surface of the aminolyzed PCL fibrous scaffolds. Table 1 shows the

detectable amount in terms of the areal density of the amino groups on the surface of the aminolyzed PCL fibrous scaffolds as a function of the initial concentration of the HMD/IPA solution used during the aminolysis. Without the presence of HMD, amino groups could not be detected. In the presence of HMD, the average areal density of the amino groups increased from 0.20×10^{-8} mol · cm^{-2} at 1 M HMD to 1.22×10^{-8} mol · cm^{-2} at 4 M HMD and finally to 1.28×10^{-8} mol · cm^{-2} at 5 M HMD. The wettability of the surface of the aminolyzed PCL fibrous scaffolds with respect to that of the neat PCL fibrous scaffolds in terms of the advancing/receding water contact angles was further investigated, and the results are also shown in Table 1. Both of the water contact angle values decreased with an increase in the extent of aminolysis, i.e., from 142°/86° for the neat PCL fibrous scaffolds to 124−125°/71−72° for the ones aminolyzed with 4 and 5 M HMD, respectively. Apparently, the aminolytic treatment with 4 M HMD was ample to effectively introduce a relatively high density of amino groups on the surface of the PCL fibrous scaffolds.

The introduction of amino groups on the surface of the PCL fibrous scaffolds not only improved the hydrophilicity of the surface but also provided necessary active sites upon which biomolecules such as collagen (i.e., marine collagen, COLM; type I collagen, COLI; type IV collagen, COLIV), chitosan (i.e., CS15, M_w = 15 000 g · mol^{-1}; CS83, M_w = 83 000 g · mol^{-1}), or GRGDS peptide (i.e., H-Gly-Arg-Cly-Asp-Ser-OH) could be further immobilized. As mentioned, the attached amino groups were first activated with DSC, with *N*-hydroxysuccinimide being lost from the reaction, and the as-formed succinimidyl esters were later reacted with each of the selected biomolecules, with *N*-hydroxysuccinimide again being cleaved from the reaction. The PCL fibrous scaffolds that had been aminolyzed with 4 M HMD were used in the subsequent immobilization with biomolecules. After the aminolyzed PCL fibrous scaffolds had been activated with DSC, their surface became more hydrophobic, as evidenced by the advancing/receding water contact angles of 136°/78° (see Table 2), which confirmed the existence of the hydrophobic *N*-succinimidyl groups. After immobilization with the biomolecules, the surfaces became more hydrophilic once again, with both of the water contact angle values decreasing to 122−127°/0°. The average areal density of the amino groups on the surface of the biomolecule-immobilized PCL fibrous scaffolds was in the range of 4.9×10^{-10}−9.3×10^{-10} mol · cm^{-2}, with the COLM-immobilized PCL fibrous scaffolds exhibiting the greatest value and the GRGDS-immobilized ones exhibiting the least.

ATR-FTIR was used to investigate the chemical functional groups that were present on the surfaces of the neat and modified PCL fibrous scaffolds, and the results are shown in Figure 2. There was a major absorption peak corresponding to the carbonyl ester of the neat PCL fibrous scaffolds at 1720 cm^{-1}. No signals due to the N−H stretching of the amino groups or the carbonyl (C═O) stretching of the amide linkage were, however, observed for the aminolyzed PCL fibrous scaffolds. This could be a result of the extremely low concentration of −NH_2 groups available for detection by the instrument (viz., the sampling depth of ATR-FTIR was ~1−2 μm). For the activated, aminolyzed PCL fibrous scaffolds, no evidence for the C═O stretching of the succinimidyl esters was observed. Once again, this could be a result of the extremely low concentration of chemical species on the surface of the materials. Nonetheless, after immobilization with the biomolecules, the absorption peaks at 1640 cm^{-1} associated with the C═O stretching of amide I and at 1560 cm^{-1} associated with the N−H bending of amide II appeared

Table 2. Areal Density of Amino Groups on the Surface of the Aminolyzed PCL Fibrous Scaffolds as a Function of the HMD Concentration and the Resulting Advancing and Receding Water Contact Angles of the Surfaces

		water contact angle		
sample	NH_2 concn (mol · cm^{-2})	advancing (deg)	receding (deg)	hysteresis (deg)
neat PCL		142 ± 2	86 ± 2	56
aminolyzed PCL[a]	$1.22 \pm 0.02 \times 10^{-8}$	124 ± 2	71 ± 2	53
activated, aminolyzed PCL		136 ± 3	78 ± 2	58
COLM-PCL[b]	$9.3 \pm 0.9 \times 10^{-10}$	123 ± 3	0	123
COLI-PCL[b]	$7.1 \pm 0.9 \times 10^{-10}$	122 ± 2	0	122
COLIV-PCL[b]	$6.6 \pm 1.6 \times 10^{-10}$	125 ± 3	0	125
CS15-PCL[b]	$5.5 \pm 0.9 \times 10^{-10}$	127 ± 2	0	127
CS83-PCL[b]	$6.0 \pm 2.5 \times 10^{-10}$	125 ± 2	0	125
GRGDS-PCL[b]	$4.9 \pm 1.6 \times 10^{-10}$	122 ± 3	0	122

[a] The scaffolds were aminolyzed with a 4 M HMD solution for 8 h. [b] Acronyms: COLM, marine collagen; COLI, type I collagen; COLIV, type IV collagen; CS15, chitosan with M_w = 15 000 g · mol^{-1}; CS83, chitosan with M_w = 83 000 g · mol^{-1}; GRGDS, peptide sequence HGly-Arg-Cly-Asp-Ser-OH.

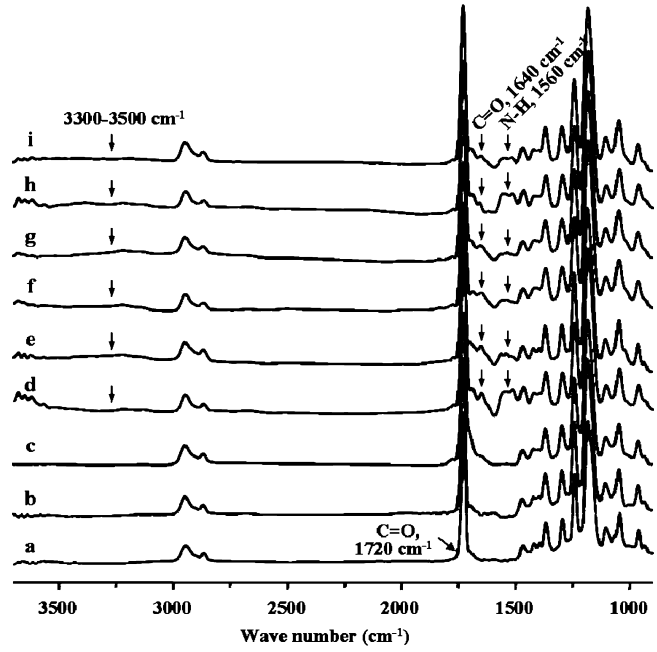

FIGURE 2. ATR-FTIR spectra of (a) the neat PCL fibrous scaffolds, (b) the aminolyzed PCL fibrous scaffolds, (c) the activated, aminolyzed PCL fibrous scaffolds, and the PCL fibrous scaffolds that had been immobilized with (d) COLM, (e) COLI, (f) COLIV, (g) CS15, (h) CS83, and (i) GRGDS peptide. Arrows shown are for the clarity of the indicated peak positions.

in the spectra of all of the biomolecule-immobilized PCL fibrous scaffolds. Additionally, the observation of a broad peak in the range of 3000−3600 cm^{-1} corresponding to the N−H stretching of the NH_2 groups further confirmed the successful immobilization of the biomolecules on the surface of the PCL fibrous scaffolds.

3.2. Biological Evaluation of the Neat and Modified PCL Fibrous Scaffolds. ***Indirect Cytotoxicity Evaluation.*** The potential for use of the neat and modified PCL fibrous scaffolds was assessed by the indirect cytotoxicity evaluation assay, using mouse fibroblasts (L929), human epidermal keratinocytes (HEK001), and mouse preosteoblasts (MC3T3-E1) as reference cell lines. In such an evaluation, the extraction media were prepared by immersing samples in each respective culture medium for 1, 3, or 7 days. Each of the as-prepared extraction media was then used to culture each type of cell for 1 day, and the viability of the cells was compared with that of the cells that had been cultured with the respective fresh culture medium that had been preincubated for an equivalent time interval (i.e., 1, 3, or 7 days). The obtained results are shown in Figure 3. Here, the viability of the cells that had been cultured with the fresh culture media that had been preincubated for 1 day was used as the basis to obtain the relative viability values shown in the figure. Evidently, the viability of L929 for all types of PCL fibrous scaffolds was 81−90% at 1 day of immersion, 85−92% at 3 days of immersion, and 92−104% at 7 days of immersion. For HEK001, it was 73−83% at 1 day of immersion, 68−76% at 3 days of immersion, and 44−65% at 7 days of immersion. For MC3T3-E1, it was 77−84% at 1 day of immersion, 84−89% at 3 days of immersion, and 89−94% at 7 days of immersion. Obviously, the viability of both L929 and MC3T3-E1 for almost all types of the substrates, including that of the cells that had been cultured with the preincubated fresh culture media (i.e., control), increased with an increase in the immersion time in each respective medium, while an opposite trend was observed for that of HEK001. This could be due to the usual vulnerability of HEK001. The obtained results indicated nontoxicity of both the neat and modified PCL fibrous scaffolds toward the tested cell lines and suggested their applicability as cell/tissue scaffolds.

Cell Adhesion and Cell Proliferation. The potential for use of the neat and modified PCL fibrous scaffolds was further evaluated by observing their ability to support both the adhesion and proliferation of L929, HEK001, and MC3T3-E1 after having been seeded or cultured on their surfaces for 12 h or 2 or 4 days, respectively (see Figure 4). The viability of the cells that had been cultured on the surface of TCPS was used as the positive control and the viability of the cells that had been cultured on the surface of TCPS for 12 h (for each type of cell) was taken as the basis to obtain the relative viability values shown in the figure. The viability of the cells that had been cultured on any given substrate for 12 h represented the adhesion of the cells on the surface, while that of the cells that had been cultured for 2 or 4 days was taken as the proliferation of the cells on the surface.

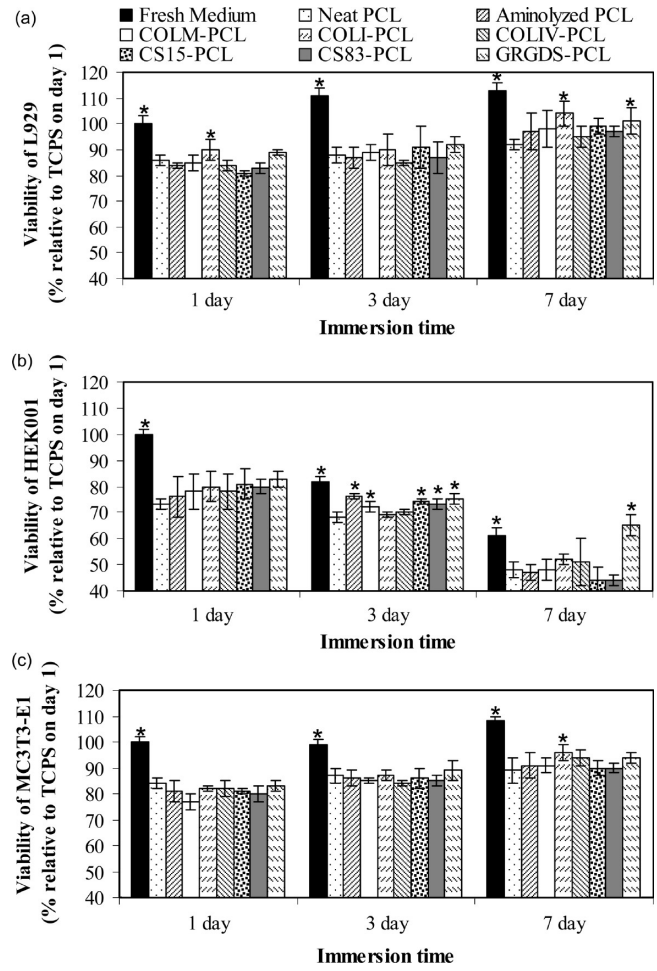

FIGURE 3. Indirect cytotoxicity evaluation of the neat and modified PCL fibrous scaffolds based on the viability of (a) mouse fibroblasts (L929), (b) human epidermal keratinocytes (HEK001), and (c) mouse preosteoblasts (MC3T3-E1) that had been cultured with the extraction media from each of these materials against the viability of the cells that had been cultured with the respective culture media for 1 day as a function of the incubation time of the extraction and the culture media of 1, 3, or 7 days. Statistical significance compared to the neat PCL fibrous scaffolds: (*) $p < 0.05$.

According to Figure 4, L929 adhered on the surface of the neat PCL fibrous scaffolds as good as they did on the surface of TCPS. The introduction of the NH_2 groups on the scaffold surface obviously improved the adhesion of the cells. The attachment of the cells on the PCL fibrous scaffold surface was further improved with the immobilization of various biomolecules, i.e., collagen, chitosan, and GRGDS peptide. Among the various biomolecule-immobilized PCL fibrous scaffolds, the COLI-immobilized PCL fibrous scaffolds provided the best support for the attachment of L929, followed by the rest of the biomolecule-immobilized substrates, which showed equivalent viability of the attached cells. On the other hand, L929 proliferated on the surface of TCPS better than they did on the surfaces of all of the PCL fibrous scaffolds. On day 2 of cell culturing, the COLI-immobilized PCL fibrous scaffolds provided the best support for the proliferation of L929, followed by almost all of the rest of the biomolecule-immobilized substrates (except for the COLM-immobilized ones). On day 4, the COLI-immobilized PCL fibrous scaffolds were still the best to support

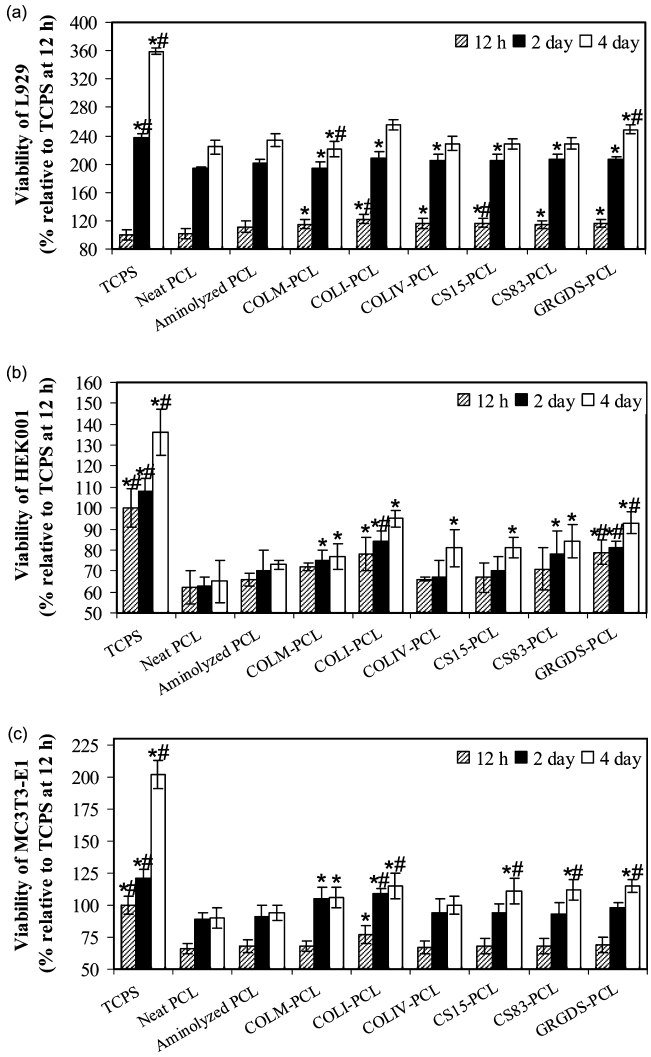

FIGURE 4. Attachment and proliferation of (a) L929, (b) HEK001, and (c) MC3T3-E1 that had been seeded or cultured on the surfaces of TCPS and the neat and modified PCL fibrous scaffolds for 12 h or 2 or 4 days. The viability of the cells that had been seeded for 12 h signifies the attachment period, while that of the cells that had been cultured for 2 and 4 days signifies the proliferation period. Statistical significance compared to the neat PCL fibrous scaffolds: (*) $p < 0.05$; (#) $p < 0.01$.

the proliferation of the cells, followed by the GRGDS-immobilized ones. At any given time point during the proliferation period, the neat and COLM-immobilized PCL fibrous scaffolds were the worst to support the proliferation of the cells.

With regard to HEK001, the surfaces of all of the PCL fibrous scaffolds were inferior in supporting the attachment and proliferation of the cells to that of TCPS. Among the various PCL fibrous scaffolds, the neat PCL substrates were obviously the worst in supporting the attachment and proliferation of HEK001. The introduction of the NH_2 groups on the scaffold surface marginally improved the adhesion of the cells. Immobilization of the scaffold surface with COLM, COLIV, CS15, and CS83 slightly improved the ability of the scaffolds in supporting the attachment and proliferation of the cells. Marked improvement was achieved with the COLI-immobilized and GRGDS-immobilized PCL fibrous scaffolds. In a similar manner, the surfaces of all of the PCL fibrous scaffolds were inferior in supporting the attachment and proliferation of MC3T3-E1 to that of TCPS. Again, among the various PCL fibrous scaffolds, the neat PCL substrates was the worst in supporting the attachment and proliferation of the cells. Among the various modified PCL fibrous scaffolds, only the COLI-immobilized PCL fibrous scaffolds provided the most significant improvement in the ability to support the attachment and proliferation of the cells. Interestingly, the ability of the GRGDS-immobilized PCL fibrous scaffolds in supporting the proliferation of MC3T3-E1 on day 4 of cell culturing was as good as that of the COLI-immobilized ones, followed by those treated with CS15 and CS83, COLM and COLIV, respectively.

Morphology of Cultured Cells. On the basis of the results shown in Figure 4, the COLI-immobilized PCL fibrous scaffolds were evidently the best in supporting the attachment and proliferation of all of the investigated cell lines. Only the SEM images of the cells that had been cultured on the surfaces of TCPS (i.e., positive control), the neat PCL fibrous scaffolds (i.e., internal control), and the COLI-immobilized PCL fibrous scaffolds are, therefore, shown in Table 3 in two different magnifications, while all of the SEM images are available as Supporting Information. Because of limited resources, morphological studies of the cultured cells were only carried out for some of the selected PCL fibrous scaffolds.

During the attachment period (i.e., at 12 h after cell seeding), the majority of L929 that had been seeded on the surfaces of all of the PCL fibrous scaffolds were still round, while those seeded on the surface of TCPS were already spreading. On the other hand, the majority of both HEK001 and MC3T3-E1 that had been seeded on TCPS and all types of scaffold surfaces were already in the spreading form. These results suggested that L929 prefers the surface of TCPS over those of the PCL fibrous scaffolds, while both HEK001 and MC3T3-E1 adhered to the PCL fibrous scaffold surfaces as well as they did on TCPS, despite the fact that the viability of the attached cells was inferior to that of the cells that had been seeded on TCPS.

On day 2 of cell culturing, the majority of L929 cultured on most of the PCL fibrous scaffolds, except for the COLI-immobilized ones, were still round, with an evidence of some spreading cells. Apparently, the shape of the spreading cells on the surfaces of most of the PCL fibrous scaffolds, including that of the COLI-immobilized ones, was spindle-like, while that of the cells on the surfaces of TCPS and GRGDS-immobilized PCL fibrous scaffolds was polygonal in nature. On day 4 of cell culturing, a significantly greater number of L929 was observed on TCPS and all types of scaffold surfaces, a result that was in line with the observed increase in the viability of the cells during the proliferation period. Interestingly, almost all of the cultured cells were spindle-like in nature, with evidence of some round cells lying on top of the spreading cells that laid down as a monolayer on the substrates. On the other hand, both HEK001 and MC3T3-E1 expanded well over the surfaces of TCPS and all types of PCL fibrous scaffolds. Similar to that

Table 3. Selected SEM Images of L929, HEK001, and MC3T3-E1 That Had Been Seeded or Cultured on the Surfaces of TCPS, the Neat PCL Fibrous Scaffolds, and the COLI-Immobilized PCL Fibrous Scaffolds for 12 h or 4 days, Respectively

Type of cells	Samples	Culturing time			
		Magnification 500x scale bar = 50 μm		Magnification 1500 - 3500x scale bar = 5 - 10 μm	
		12 h	4 d	12 h	4 d
L929	TCPS	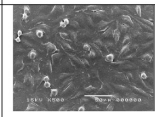	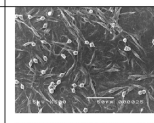	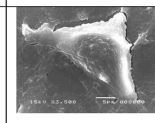	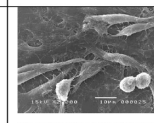
	Neat PCL	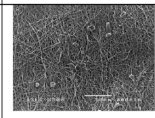	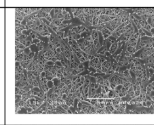	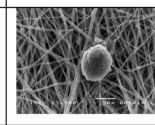	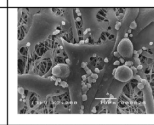
	COLI-PCL	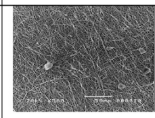	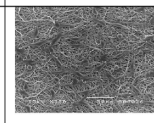	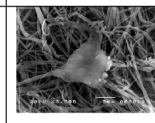	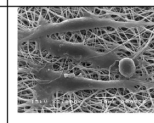
HEK001	TCPS	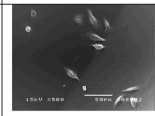	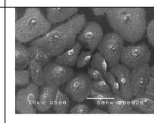	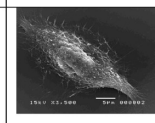	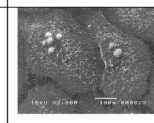
	Neat PCL	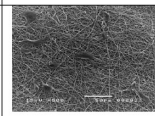	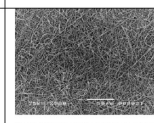	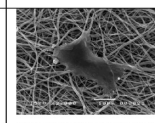	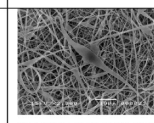
	COLI-PCL	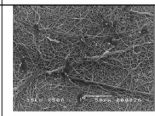	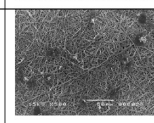	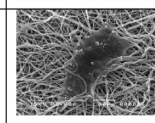	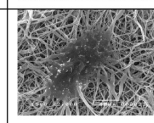
MC3T3-E1	TCPS	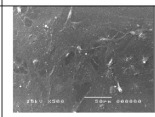	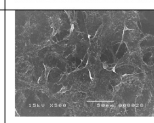	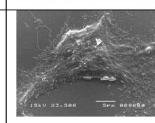	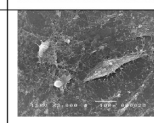
	Neat PCL	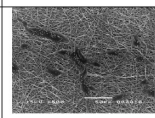	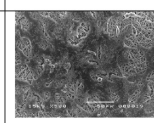	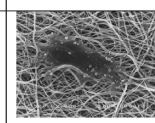	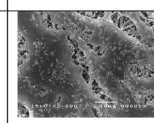
	COLI-PCL	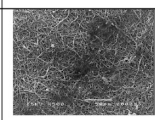	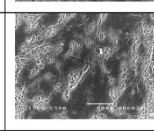	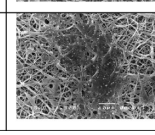	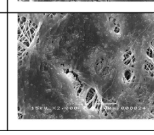

of L929, the number of HEK001 and MC3T3-E1 that was observed on day 4 was greater than that observed on day 2, a result that was in accordance with the observed increase in the viability of the cells during the proliferation period. The shape of the cultured cells was also similar to that of the cells that adhered to these surfaces after 12 h of cell seeding.

3.3. Further Discussion. Despite the inherent biodegradability and biocompatibility of PCL, the actual utilization of this material as synthetic prostheses, implants, or tissue-engineered matrixes is limited by its hydrophobicity (19), which may in vivo lead to foreign-body reactions, such as inflammation, infections, aseptic loosening, local tissue waste, and implant encapsulation (27). Approaches to further improve the biocompatibility of PCL and equivalent materials include the reduction of unspecific protein adsorption (i.e., nonfouling properties), the enhancement of specific protein adsorption, and the chemical immobilization of certain cell recognition motives on the surface of a substrate to obtain controlled interaction between the cells and the synthetic substrates (27). The improvement in the adsorption of specific proteins on the surface of a substrate could be done by the addition of some functional substances into the substrate matrix. As an effectual example, the specific adsorption of fibronectin and/or osteocalcin on hydroxyapatite (HAp) nanoparticles that had been incorporated in electrospun PCL fibrous scaffolds was postulated to be the reason for the ability of the materials to enhance the proliferation and differentiation of MC3T3-E1 in vitro (31).

Here, the chemical modification pathway was used to modify the surface of the electrospun PCL fibrous scaffolds, with an aim of improving the cytocompatibility of the materials without altering their bulk properties. Zhu et al.

(17) modified solvent-cast PCL membranes by first reacting the membranes with HMD to introduce $-NH_2$ groups on their surface. Then, the aminolyzed PCL membranes were activated with glutaraldehyde, prior to being reacted with gelatin, chitosan, or collagen. In another approach (19), the PCL membranes were first photooxidized with UV irradiation in the presence of hydrogen peroxide to impart hydroperoxide (−OOH) groups on the membrane surface. Methacrylic acid was then graft-copolymerized onto the surface of the oxidized PCL membranes under UV irradiation, prior to being reacted with gelatin. In more complicated approaches, Cheng and Teoh (8) and Sun et al. (28) utilized argon plasma and pulsed electron beam to generate peroxides (including hydroperoxides) and free radicals, respectively, on the surface of the PCL substrates. Acrylic acid was then graft-copolymerized onto the surface of the treated PCL substrates, prior to being reacted with collagen and a RGD-containing peptide, respectively. Santiago et al. (22) utilized the method proposed by Zhu et al. (17) to immobilize three different peptides [i.e., RGD, Tyr-Ile-Gly-Ser-Arg (referred to as YIGSR), and Cys-Arg-Ala-Arg-Lys-Gln-Ala-Ala-Ser-Ile-Lys-Val-Ala-Val-Ser-Ala-Asp-Arg (referred to as IKVAV)] on the surface of solvent-cast PCL disks.

Among these, the method proposed by Zhu et al. (17) was chosen for its simplicity. As shown in Table 1, the average areal density of the $-NH_2$ groups on the surface of the PCL fibrous scaffolds that had been aminolyzed with HMD for 8 h ranged from 0.20×10^{-8} to 1.28×10^{-8} mol · cm^{-2}, depending on the concentration of HMD (i.e., from 1 to 5 M). Zhu et al. (17) showed that the average areal density of the $-NH_2$ groups on the surface of the solvent-cast PCL membranes varied with the aminolyzing time (i.e., ranging from about 1.5×10^{-7} mol · cm^{-2} at 5 min to about 2.0×10^{-7} mol · cm^{-2} at 120 min). Because water contact angle measurement is a simple, yet effective method for assessing the activity of a surface, it was used to evaluate the activity of the surface of the aminolyzed PCL fibrous scaffolds. According to Table 1, the advancing/receding water contact angles of the neat PCL fibrous scaffolds were 142°/86°, which were much greater than those of the solvent-cast PCL films [i.e., 66° (sessile contact angle) (8), 81°/62° (17, 19), and 83°/67° (22)]. The large discrepancy between the water contact angles observed between the PCL fibrous scaffolds and the PCL films could be due to the roughness of the fibrous scaffold surface that enhanced the hydrophobility of the surface (i.e., the lotus effect). Recently, Chen et al. (15) showed that coating the biaxially stretched PCL membranes with electrospun PCL fibers caused the roughness of the surface to increase sharply (i.e., from about 53 nm to about 939 nm). This, in turn, was responsible for the marked increase in the sessile water contact angle, i.e., from 77° for the neat PCL membranes to 125° for the fiber-coated ones (15).

Upon aminolysis, the advancing/receding water contact angles of the PCL fibrous scaffolds that had been treated with a 4 M HMD solution for 8 h decreased to 124°/71°, which were still much greater than those of the aminolyzed PCL films (i.e., 82°/29° (17) and 78°/64° (22)). Upon immobilization of the activated, aminolyzed PCL fibrous scaffolds with the biomolecules, the average areal density of the $-NH_2$ groups on the surfaces of the biomolecule-immobilized PCL fibrous scaffolds ranged between 4.9×10^{-10} and 9.3×10^{-10} mol · cm^{-2} (see Table 2). Among the various biomolecule-immobilized PCL fibrous scaffolds, the ones immobilized with COLM exhibited the greatest value, followed by the ones immobilized with COLI, with those immobilized with GRGDS peptide exhibiting the lowest value. Even though the advancing water contact angles of these biomolecule-immobilized PCL fibrous scaffolds (i.e., 122−127°) were similar to that of the aminolyzed ones (i.e., 124°), the receding water contact angles of these scaffolds were much lower (i.e., 0° as compared with 71°). The much larger hysteresis observed for the biomolecule-immobilized PCL fibrous scaffolds (i.e., 122−127°) as compared with the aminolyzed ones (i.e., 53°) should be a result of the conformational reorganization of the immobilized biomolecules upon their prior exposure to water (17, 32) because the hydrophilic parts of the biomolecules would reorient to generate a hydrophilic surface in response to the prior contact with the water molecules.

On the other hand, such a complete wettability was not observed for the biomolecule-immobilized PCL films (17, 22) because the receding water contact angles were found to be in the range of 9.8−12.2° for the PCL films that had been immobilized with chitosan, gelatin, and collagen (17) and of 49.1−60.6° for the ones that had been immobilized with RGD, YIGSR, and IKVAV peptides (22). The difference in the wetting behavior of the surfaces of the biomolecule-immobilized PCL fibrous scaffolds and the biomolecule-immobilized PCL films upon their prior exposure to water could be due to the difference in the topographical nature of these two different substrates because the capillary action could play a major role in enhancing the water absorption of the biomolecule-immobilized PCL fibrous scaffolds once the surface of the individual fiber segments became amply hydrophilic. Chen et al. (15) showed that the hydrophilicity of the PCL surface could be enhanced by a simple treatment with NaOH. Between the neat and fiber-coated PCL membranes that had been treated with a 5 M NaOH solution, the fiber-coated ones exhibited a complete wettability because their sessile water contact angle was 0° compared with 60° of the neat PCL membranes, which was due to the capillary action induced by the coated fibers (15).

With regard to the cell culture studies, a number of ECM proteins, e.g., bone sialoprotein, collagen, fibronectin, laminin, osteopontin, tenascin, thrombospondin, vitronectin, and von Willebrand factor, that contain the cell-binding domain RGD have been known to play a critical role in cell behavior because they regulate gene expression by signal transduction set in motion by cell adhesion to a functional biomaterial (27, 33, 34). In type I and IV collagens (i.e., COLI and COLIV, respectively), the RGD sequence may be cryptic in their native form and only becomes exposed upon proteolytic degradation and denaturation (35, 36). The process

of integrin-mediated cell adhesion consists of a cascade of four different, partly overlapping events (27, 37): cell attachment, cell spreading, organization of the actin cytoskeleton, and formation of focal adhesions. On the basis of these previous reports, it is expected that immobilization of the electrospun PCL fibrous scaffolds with RGD-containing peptides as well as one of the above-mentioned RGD-expressing ECM proteins, particularly COLI, should enhance the cytocompatibility of the materials appreciably.

According to the results shown in Figure 4, the COLI-immobilized PCL fibrous scaffolds were clearly the best in supporting the attachment and proliferation of all of the investigated cell types, followed by the GRGDS-immobilized ones. Between the COLI- and GRGDS-immobilized PCL fibrous scaffolds, the larger size and the greater content of the immobilized COLI could provide better accessibility to cells, hence the observed better cytocompatibility of the COLI-immobilized PCL fibrous scaffolds than the GRGDS-immobilized ones. To be more explicit, because the texture of these scaffolds is fibrous in nature, not all of the immobilized biomolecules are exposed to the cells (e.g., the ones that were on the surface of the underlying fibers). As a result, the accessibility of the immobilized biomolecules should depend on their molecular weights (i.e., their size) because the larger biomolecules, e.g., COLI in our case, should be more accessible than the shorter ones, e.g., GRGDS peptide. In fact, the ability of the COLI-immobilized PCL fibrous scaffolds to best support the attachment and proliferation of L929 and MC3T3-E1 is somewhat expected because COLI is the major collagen-based protein synthesized by fibroblasts and osteoblasts (27, 33, 38). For HEK001, despite their inability to synthesize COLI, the locomotion of keratinocytes on COLI was shown to be RGD-mediated (39). Despite the fact that keratinocytes are capable of synthesizing COLIV but not COLI (39), the relatively poor ability of the COLIV-immobilized PCL fibrous scaffolds to support the attachment and proliferation of HEK001 with respect to that of the COLI-immobilized ones should be due to less exposure of the RGD-binding sequence of the immobilized COLIV as compared with the immobilized COLI (35, 36).

As mentioned, chemical modification by immobilization of certain cell recognition motives on the surface of a substrate is not the only means to enhance the biocompatibility of the substrate; the adsorption of either unspecific or specific proteins also plays a major role (27). Van Wachem et al. (40) showed that fibronectin, a RGD-expressing protein, preferentially adsorbed on the hydrophilic surface of TCPS better than the hydrophobic surfaces of poly(ethylene terephthalate) and the adsorption of the protein influenced greatly the adhesion of human endothelial cells. Comparatively, the surfaces of both the neat and modified PCL fibrous scaffolds are more hydrophobic than that of TCPS. The adsorption of both the collagenous and noncollagenous proteins synthesized by L929, HEK001, and MC3T3-E1 during their attachment and proliferation processes should occur to a much greater extent on the hydrophilic surface of TCPS than on the more hydrophobic surfaces of the fibrous scaffolds (viz., not to mention about another complication that rises from the highly porous nature of the fibrous scaffolds that could cause the proteins secreted by the cells to be drain away and become unexposed to the cells). This, therefore, is the likely reason for the observed greatest ability of TCPS to support the attachment and proliferation of all of the investigated cell types (see Figure 4).

4. CONCLUSION

Immobilization of various biomolecules, e.g., collagen, chitosan, and GRGDS peptide, on the surface of the electrospun PCL fibrous scaffolds was carried out in this study. First, the amino groups were introduced on the scaffold surface as a result of chemical treatment with HMD. Second, the introduced amino groups were used as precursors for subsequent immobilization with the biomolecules. ATR-FTIR data confirmed the existence of the immobilized biomolecules, while the dynamic water contact angle data indicated that the surfaces of the biomolecule-immobilized PCL fibrous scaffolds were more hydrophilic than those of the untreated ones. The potential for use of the neat, aminolyzed, and biomolecule-immobilized PCL fibrous scaffolds for tissue and/or cell culture was assessed with three different cell lines, e.g., mouse fibroblasts (L929), human epidermal keratinocytes (HEK001), and mouse calvaria-derived preosteoblastic cells (MC3T3-E1). Indirect cytotoxicity evaluation revealed that both the neat and modified PCL fibrous scaffolds released no substances in levels that were harmful to these cells. Among the various biomolecule-immobilized PCL fibrous scaffolds, the ones that had been immobilized with type I collagen, a RGD-containing protein, showed the greatest ability to support the attachment and proliferation of all of the investigated cell types, followed by those that had been immobilized with GRGDS peptide. However, the ability of these PCL fibrous scaffolds to support the attachment and proliferation of the cells was inferior to that of TCPS.

Acknowledgment. This research work was supported, in part, by (1) The Thailand Research Fund through the Master Research Grants program (TRG-MRG; MRG475S016), (2) The National Research Council of Thailand through the research program "Multidisciplinary Research Series in Tissue Engineering of Skin", and (3) The Center for Petroleum, Petrochemicals and Advanced Materials. Associate Professor Dr. Prasit Pavasant is acknowledged for donation of the mouse calvaria-derived preosteoblastic cells (MC3T3-E1) used in this study. Associate Professor Dr. Sanong Ekgasit is acknowledged for access to the ATR-FTIR research facility.

Supporting Information Available: Additional experimental detail, data, and results. This material is available free of charge via the Internet at http://pubs.acs.org.

REFERENCES AND NOTES

(1) Rho, K. S.; Jeong, L.; Lee, G.; Seo, B. M.; Park, Y. J.; Hong, S. D.; Roh, S.; Cho, J. J.; Park, W. H.; Min, B. M. *Biomaterials* **2006**, *27*, 1452–1461.

(2) Suwantong, O.; Waleetorncheepsawat, S.; Sanchavanakit, N.; Pavasant, P.; Cheepsunthorn, P.; Bunaprasert, T.; Supaphol, P. *Int. J. Biol. Macromol.* **2007**, *40*, 217–223.

(3) Chen, G.; Ushida, T.; Tateishi, T. *Macromol. Biosci.* **2002**, *2*, 67–77.
(4) Coombes, A. G. A.; Verderiob, E.; Shawa, B.; Lib, X.; Griffinb, M.; Downes, S. *Biomaterials* **2002**, *23*, 2113–2118.
(5) Masuko, T.; Iwasaki, N.; Yamane, S.; Funakoshi, T.; Majima, T.; Minami, A.; Ohsuga, N.; Ohta, T.; Nishimura, S. I. *Biomaterials* **2005**, *26*, 5339–5347.
(6) Boccafoschi, F.; Habermehl, J.; Vesentini, S.; Mantovani, D. *Biomaterials* **2005**, *26*, 7410–7417.
(7) Neamnark, A.; Sanchavanakit, N.; Pavasant, P.; Bunaprasert, T.; Supaphol, P.; Rujiravanit, R. *Carbohydr. Polym.* **2007**, *68*, 166–172.
(8) Cheng, Z.; Teoh, S. H. *Biomaterials* **2004**, *25*, 1991–2001.
(9) Ng, C. S.; Teoh, S. H.; Chung, T. S.; Hutmacher, D. W. *Polymer* **2000**, *41*, 5855–5864.
(10) Coombes, A. G. A.; Rizzi, S. C.; Williammson, M. R.; Barralet, J. E.; Downes, S.; Wallace, W. A. *Biomaterials* **2004**, *25*, 315–325.
(11) Ng, K. W.; Hutmacher, D. W.; Schantz, J. T.; NG, C. S.; Too, H.; Lim, T. C.; Phan, T. T.; Teoh, S. H. *Tissue Eng.* **2001**, *7*, 441–455.
(12) Khor, H. L.; Ng, K. W.; Schantz, J. T.; Phan, T. T.; Lim, T. C.; Teoh, S. H.; Hutmacher, D. W. *Mater. Sci. Eng. C* **2002**, *20*, 71–75.
(13) Dai, N. T.; Williammson, M. R.; Khammo, N.; Adams, E. F.; Coombes, A. G. A. *Biomaterials* **2004**, *25*, 4263–4271.
(14) Hutmacher, D. W.; Schantz, T.; Zein, I.; Ng, K. W.; Teoh, S. H.; Tan, K. C. *J. Biomed. Mater. Res.* **2001**, *55*, 203–216.
(15) Chen, F.; Lee, C. N.; Teoh, S. H. *Mater. Sci. Eng. C* **2007**, *27*, 325–332.
(16) Ma, Z.; Gao, C.; Ji, J.; Shen, J. *Eur. Polym. J.* **2002**, *38*, 2279–2284.
(17) Zhu, Y.; Gao, C.; Liu, X.; Shen, J. *Biomacromolecules* **2002**, *3*, 1312–1319.
(18) Zhu, Y.; Gao, C.; Liu, X.; Shen, J. *J. Biomed. Mater. Res. A* **2004**, *69*, 436–443.
(19) Zhu, Y.; Gao, C.; Shen, J. *Biomaterials* **2002**, *23*, 4889–4895.
(20) Zhu, Y.; Gao, C.; He, T.; Shen, J. *Biomaterials* **2004**, *25*, 423–430.
(21) Matsuda, A.; Kobayashi, H.; Itoh, S.; Kataoka, K.; Tanaka, J. *Biomaterials* **2005**, *26*, 2273–2279.
(22) Santiago, L. Y.; Nowak, R. W.; Rubin, J. P.; Marra, K. G. *Biomaterials* **2006**, *27*, 2962–2969.
(23) Koh, H. S.; Yong, T.; Chan, C. K.; Ramakrishna, S. *Biomaterials* **2008**, *29*, 3574–3582.
(24) Wang, X. H.; Li, D. P.; Wang, W. J.; Feng, Q. L.; Cui, F. Z.; Xu, Y. X.; Song, X. H. *Int. J. Biol. Macromol.* **2003**, *33*, 95–100.
(25) Ding, Z.; Chen, J.; Gao, S.; Chang, J.; Zhang, J.; Kang, E. T. *Biomaterials* **2004**, *25*, 1059–1067.
(26) Liao, J. D.; Lin, S. P.; Wu, Y. T. *Biomacromolecules* **2005**, *6*, 392–399.
(27) Hersel, U.; Dahmen, C.; Kessler, H. *Biomaterials* **2003**, *24*, 4385–4415.
(28) Sun, H.; Wirsen, A.; Albertsson, A. C. *Biomacromolecules* **2004**, *5*, 2275–2280.
(29) Wutticharoenmongkol, P.; Sanchavanakit, N.; Pavasant, P.; Supaphol, P. *Macromol. Biosci.* **2006**, *6*, 70–77.
(30) Aziz, D. M. *Anim. Reprod. Sci.* **2006**, *92*, 1–8.
(31) Wutticharoenmongkol, P.; Pavasant, P.; Supaphol, P. *Biomacromolecules* **2007**, *8*, 2602–2610.
(32) Roudman, A. R.; DiGiano, F. A. *J. Membr. Sci.* **2000**, *175*, 61–73.
(33) Hernández-Gil, I. F.-T.; Gracia, M. A. A.; Pingarrón, M. D. C.; Jerez, L. B. *Med. Oral, Patología Oral Cirugía Bucal* **2006**, *11*, E47—51.
(34) Li, J.; Yun, H.; Gong, Y.; Zhao, N.; Zhang, X. *Biomacromolecules* **2006**, *7*, 1112–1123.
(35) Davis, G. E. *Biochem. Biophys. Res. Commun.* **1992**, *182*, 1025–1031.
(36) Xu, J.; Rodriguez, D.; Petitclerc, E.; Kim, J. J.; Hangai, M.; Yuen, S. M.; Davis, G. E.; Brooks, P. C. *J. Cell Biol.* **2001**, *154*, 1069–1079.
(37) Lebaron, R. G.; Athanasiou, K. A. *Tissue Eng.* **2000**, *6*, 85–103.
(38) Mano, J. F.; Silva, G. A.; Azevedo, H. S.; Malafaya, P. B.; Sousa, R. A.; Silva, S. S.; Boesel, L. F.; Oliveira, J. M.; Santos, T. C.; Marques, A. P.; Neves, N. M.; Reis, R. L. *J. R. Soc. Interface* **2007**, *4*, 999–1030.
(39) Kim, J. P.; Zhang, K.; Kramer, R. H.; Schall, T. J.; Woodley, D. T. *J. Invest. Dermatol.* **1992**, *98*, 764–770.
(40) Van Wachem, P. B.; Vreriks, C. M.; Beugeling, T.; Feijen, J.; Bantjes, A.; Detmers, J. P.; van Aken, W. G. *J. Biomed. Mater. Res.* **1987**, *21*, 701–718.

AM900048T